Accepted Manuscript

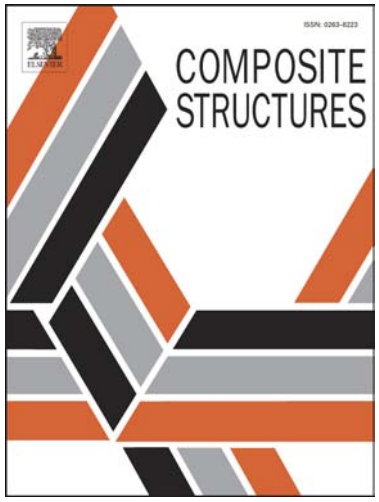

Experimental investigation on the energy absorption and contact force of unstiffened and grid-stiffened composite cylindrical shells under lateral compression

Majid Moeinifard, Gholamhossein Liaghat, Gholamhossein Rahimi, Ali Talezadehlari, Homayoun Hadavinia

PII: S0263-8223(16)30689-4
DOI: http://dx.doi.org/10.1016/j.compstruct.2016.05.067
Reference: COST 7480

To appear in: *Composite Structures*

Received Date: 29 November 2015
Revised Date: 11 April 2016
Accepted Date: 23 May 2016

Please cite this article as: Moeinifard, M., Liaghat, G., Rahimi, G., Talezadehlari, A., Hadavinia, H., Experimental investigation on the energy absorption and contact force of unstiffened and grid-stiffened composite cylindrical shells under lateral compression, *Composite Structures* (2016), doi: http://dx.doi.org/10.1016/j.compstruct.2016.05.067

Experimental investigation on the energy absorption and contact force of unstiffened and grid-stiffened composite cylindrical shells under lateral compression

Majid Moeinifard[a], Gholamhossein Liaghat[a,b*], Gholamhossein Rahimi[a], Ali Talezadehlari[a], Homayoun Hadavinia[b]

[a] Faculty of Mechanical Engineering, Tarbiat Modares University, P.O.Box 15115-111, Tehran, Iran.

[b] School of Mechanical and Automotive Engineering, Kingston University, London, U.K.

Abstract

In this paper, two different types of unstiffened and lozenge grid-stiffened E-glass/Epoxy composite cylindrical shells are experimentally investigated under lateral compression. The composite shells are compressed in two different loading conditions; between two rigid flat platens and between a rigid flat platen and a rigid cylindrical indenter which is aligned perpendicular to the shell axis. The effects of the grid stiffeners on the stiffness, contact force and energy absorption capacity of the composite cylindrical shells are investigated in the two mentioned loading conditions. Incorporation of grid stiffeners in the composite cylindrical shells leads to an increase in the structural stiffness, contact force and energy absorbing capacity in both loading conditions. Furthermore, it is observed that the effect of the stiffeners on the structural stiffness is dominant in the elastic deformation stage of the compression processes. The results show that stiffening the composite cylindrical shells with lozenge grid stiffeners can increase the specific energy absorption almost twice in comparison with the unstiffened composite shells; and among all of the specimens, the grid-stiffened structures compressed between two rigid flat platens have the highest specific energy absorption, while the unstiffened structures compressed by the cylindrical indenter have the least capacity to absorb energy.

*Corresponding author at: Faculty of Mechanical Engineering, Tarbiat Modares University, P.O. Box 75914–353, Tehran, Iran. Tel: +98-2182883387
E–mail address: Ghlia530@modares.ac.ir (Gh. Liaghat).

Keywords: composite shell, grid-stiffened, lateral compression, contact force, energy absorption.

1. Introduction

Energy absorbing structures are widely used in many applications such as in automotive, aero-space, building, shipping, oil and gas industries. The most important features of these kinds of structures can be mentioned as high energy absorbing capacity, low weight etc. Metallic energy absorbing structures under different loading conditions were widely investigated by many researchers. Under different loading conditions, these kinds of structures, as energy absorbing structures, may undergo several different processes such as folding, inversion, flattening, splitting processes and so on. For example, circular thin-walled tubes under axial and lateral compressions are investigated by many researchers [1-6]. Alghamdi [7] and Olabi et al. [8] presented reviews of the collapsible impact energy absorbers and the metallic energy absorbing structures, respectively. The lateral compression of thin-walled metallic structures was investigated by Olabi et al. [9] by using the nested circular tube energy absorbers under lateral impact loading. Morris et al. [10] presented an experimental and numerical investigation on the nested circular and elliptical type energy absorbers. In their work, nested systems consist of circular tubes or elliptical shaped tubes of different diameters which were placed within each other and their axes being parallel. They also discussed how the circular tubes were transformed into elliptical shapes and how such a modified shape exhibited greater crushing efficiencies than their circular shaped counterparts.

Niknejad et al. investigated experimentally the crushing behavior of the empty and polyurethane foam-filled brazen tubes, [12]. They observed that polyurethane foam filler can considerably increase the specific energy absorption of the thin-walled structures. Their results showed the formation of two or in some cases four, plastic hinges in the specimens depends on the geometrical dimensions of the specimens. Their theoretical model reasonably predicts the load-displacement behavior of the rectangular [13] and hexagonal [14] metallic tubular structures under lateral quasi-static compression, in comparison with the experimental data.

Aluminum foam-filled and empty tubes made of aluminum, brass and titanium during the lateral compression was studied by Hall et al. [15]. Estimation based on initial crushing loads showed that for comparable energy absorption, filled tubes are lighter than thicker empty tubes. Fan et al. [16] demonstrated the advantage of sandwich tube. They studied experimentally the deformation behavior of sandwich tubes under quasi-static lateral crushing. Their results showed that tubes filled by aluminum foam tend to change the deformation mode of empty tubes from a non- sequential to a sequential folding mode due to the plateau region of the foam.

Composite structures are also extensively used in different energy absorbing and buckling resistant applications, due to to high specific strength and specific energy absorption capabilities. Improvements in manufacturing technologies have contributed in increasing the rates of production during the reinforcement-matrix association, notably because of high quality and reliability of the filament winding process, resin transfer molding (RTM) and other techniques. In the past two decades, these types of energy absorbing structures were widely investigated by many researches. Taher et al. [17] experimentally evaluated the crashworthiness characteristics of a novel design for cost-effective crashworthy composite glass fiber- reinforced plastic sandwich structures. They described the design, manufacturing and crush testing of rectangular fabricated blocks. Palanivelu et al. [18] presented an experimental investigation of quasi-static crushing behavior of nine different geometrical shapes of small-scale composite tubes. Their main idea was to understand the effect of geometry, dimension and triggering mechanism on the progressive deformation of small-scale composite tubes. They found that the crushing characteristics and the corresponding energy absorption of the special geometrical shapes are better than the standard geometrical shapes such as square and hexagonal cross sections. Furthermore, they concluded that the tulip triggering

attributed to a lower peak crush load followed by a steady mean crush load compared to the 45° chamfering triggering profile which resulted into a higher energy absorption in most of the geometrical shapes of the composite tubes.

Chiu et al. [19] investigated the response of a tulip-triggered cylindrical energy absorbing structure undergoing crushing at increasing strain rates. In their work, the energy absorption was found to be independent of strain rate as the total energy absorption appeared to be largely associated with fiber-dominated fracture, which is independent of strain rate within the studied range.

Tarlochan et al. [20] investigated the crushing response of composite sandwich structures under quasi-static compressive loads. In their work, the mechanism of progressive crushing of the sandwich structures and its relation to the energy absorption capabilities was deliberated. The aim of their study was to design and fabricate tubular sandwich structures that have potential as energy absorber devices under the axial loading.

The stability of crushing process is of great interest in automotive applications. Mahdi and Sebaey [21] studied quasi-static crushing behavior of composite tubes with four different cross-sections to find the best cross-section in terms of the crushing load and the energy-absorption capacities. Their results showed that introducing the geometrical reinforcement inside the tubes could have a positive effect on the stability of the crushing process during the loading, the average crush load, and the crush-load efficiency.

Investigation of composite structures under lateral loading conditions has also received great deal of attention. For instance, Gupta and Abbas [22] presented an experimental investigation on the flattening of cylindrical composite tubes. They studied the effects of geometrical parameters (i.e. the diameter to thickness ratio) on the peak crushing load, post collapse load, energy absorption and deformation behavior of the specimens. Also, they derived a theoretical formulation in order to predict the load- displacement behavior of the tubes in two different stages of elastic and fracture lines in the progressive fracture of multiple numbers of plies in each tube. Their results showed a reasonable agreement between the theoretical and experimental results.

Calme et al. [23] studied experimentally and numerically the flattening process in the carbon-epoxy cylindrical rings made by resin transfer molding by association of braided three-dimensional tubular preforms with DGEBA-IPD resin. In the linear region, the analytical modeling of elastic stresses giving the distribution of hoop and transverse shear stresses were validated by finite element simulation. In the elastic–plastic domain, energy absorption in 3D rings was modeled by a phenomenological approach. The proposed energy absorption model for non-linear 3D rings showed a good correlation with experiments. They concluded that the superiority of the 3D solution allows avoiding delamination problems during the lateral crushing. Abosbaia et al. [24] experimentally studied the effects of segmentation on the crushing behavior of laterally compressed composite tubes. They found that, segmented composite tubes, consisting of cotton fiber/epoxy and carbon fiber/epoxy are particularly efficient crush elements and segmented composite tubes including tissue mat glass fibers were found to suffer from low energy absorption.

Mahdi and El Kadi [25] investigated the composite elliptical tubes experimentally and by using artificial neural networks (ANN) technique they predicted the crushing behavior and energy absorption characteristics of laterally loaded glass fiber/epoxy composite elliptical specimens. Their predicted results were compared with experimental data in terms of load carrying capacity and energy absorption capability which showed good agreement. They concluded that, ANN techniques could effectively be used to predict the response of collapsible composite energy absorber devices subjected to different loading conditions. Also, as is the case for experimental findings, their predictions obtained using ANN showed the significant effect of the ellipticity ratio on the crushing behavior of laterally loaded tubes.

Experimental investigation on the flattening process of the empty and polyurethane foam-filled E-glass/vinyl ester composite tubes is presented by Niknejad et al. [26]. Their results showed that the presence of polyurethane foam inside the composite tubes suppresses the circumferential delimitation process and fiber fracturing and consequently, increases the specific absorbed energy by the composite tubes during the flattening process. Also, they observed that, injection of the polyurethane foam in the composite tubes causes the more regular deformation mode, comparing with

the empty composite tubes. Hafeez and Almaskari [27] studied the filament wound cylindrical glass reinforced epoxy (GRE) tubes subjected to lateral indentation, supported by V shaped cradles at each end. It was concluded that specimen resting on V support experience higher loads and bigger damage area for same indentation displacement, which is in contrary to the observation already made in literature for semi-circular cradle supported specimens.

Grid-stiffened structures are known as ultra-light structures that are used in applications where the structure mass is a key design factor, such as in automotive and aero-space industries. These kinds of structures have many advantages such as high strength and stiffness to weight ratios and damage tolerance. The grid of stiffening ribs is the primary feature in these structures and filament winding is employed as the most convenient manufacturing technique.

Kim [28] investigated reliability of a postbuckled composite isogrid stiffened shell structure under a compression load. His results showed that the postbuckled cylinder continued to resist compression loading even after one or more stiffeners fractured. The testing evaluation revealed that the stiffener buckling was the critical failure mode and it was demonstrated to be tolerant to structural damage due to the multiplicity of load paths. He also found that the skin resisted radial displacements and increased the axial stiffness of the cylinder.

Kidane [29] analyzed the buckling behavior of grid stiffened composite structures by theoretical, experimental and numerical approaches. He studied the effects of skin thickness, skin winding angle, stiffener orientation angle and longitudinal modulus on the buckling load of these structures. His results demonstrated that the variation in shell winding angle had different effects on stiffened cylinders failing in different failure modes; for a stiffened cylinder failing in local skin buckling failure mode, increase in winding angle decreased the load resistance of the structure, while for a stiffened cylinder failing in stiffener crippling failure mode, improvement in load resistance was noted with increase in shell winding angle. Furthermore, based on his results, for a stiffened cylinder failing in global buckling failure mode, an optimum shell-winding angle of 54° was observed. Also, he observed that increase in skin thickness increased the buckling resistance of the stiffened structure continuously, while an optimum skin thickness of 2.2 mm was resulted in the highest specific buckling load.

Zhang et al. [30] developed a progressive failure methodology to simulate the initiation and propagation of multi-failure modes for advanced grid stiffened (AGS) composite plates/shells on the basis of a stiffened element model. The methodology was able to simulate initiation and propagation process of multi-mode failures based on a set of 2D stress-based polynomial failure criteria. An equivalent degraded stiffness rule after delamination was deduced, which can weaken the ability of buckling resistance but have a little influence on the in-plane load-carrying ability.

The complete cycle of manufacturing and testing of three different types of cylindrical structures; unstiffened shell, lattice cylinder and grid-stiffened shell with the emphasis on the stiffened structures were presented by Buragohain and Velmurugan [31]. They concluded that the efficiency of these structures was greatly enhanced by the stiffening ribs and, as reflected by the highest specific buckling loads, the grid-stiffened shells, especially the lattice cylinders, remain the most efficient structure.

Yazdani et al. [32] investigated experimentally the buckling behavior of unstiffened and stiffened shells with hexagonal, triangular and lozenge grids manufactured by a special-designed filament winding machine. Based on their experimental results, the critical buckling load was higher for the shells with hexagonal and triangular grids while the unstiffened shells and stiffened shells with lozenge grids exhibited much lower critical buckling loads. Furthermore, they observed that in very small skin thicknesses, when the specific buckling loads for all specimens were compared, the unstiffened shells showed the highest specific buckling load.

In the present work, unstiffened and grid-stiffened composite cylindrical shells under compression loads applied by either between two flat plates or a rigid cylindrical indenter that is aligned perpendicular to the specimen axis and a flat platen are investigated experimentally. To the best of our knowledge, this is the first investigation on the flattening and indentation of the grid-stiffened composite cylindrical structures with the focus on their energy absorption and deformation behavior under quasi-static compression load.

2. Experimental Studies

2.1. Materials

The composite shells were fabricated from E-glass fibers and an epoxy matrix by mixing of CY-219 epoxy and HY-5161hardner with a mixing ratio of 2:1, respectively. A wax release agent was used three times in order to easily separate the outer mold parts and the specimens.

The material properties of the glass fiber and epoxy matrix were obtained by performing standard tensile tests according to ASTM D-2256 and D-638 standards, respectively. Typical load-displacement curve and engineering stress-strain curve obtained from the fiber and matrix are shown in Figs. 1 and 2. Tables 1 and 2 show the material properties of the fiber and matrix, respectively.

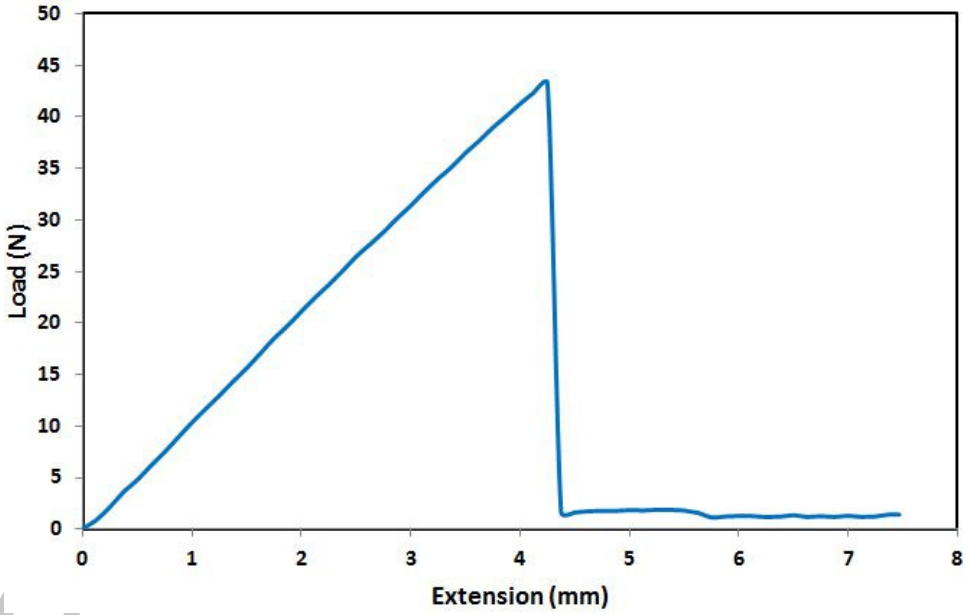

Fig 1. A typical load-extension diagram of the E-Glass fibers.

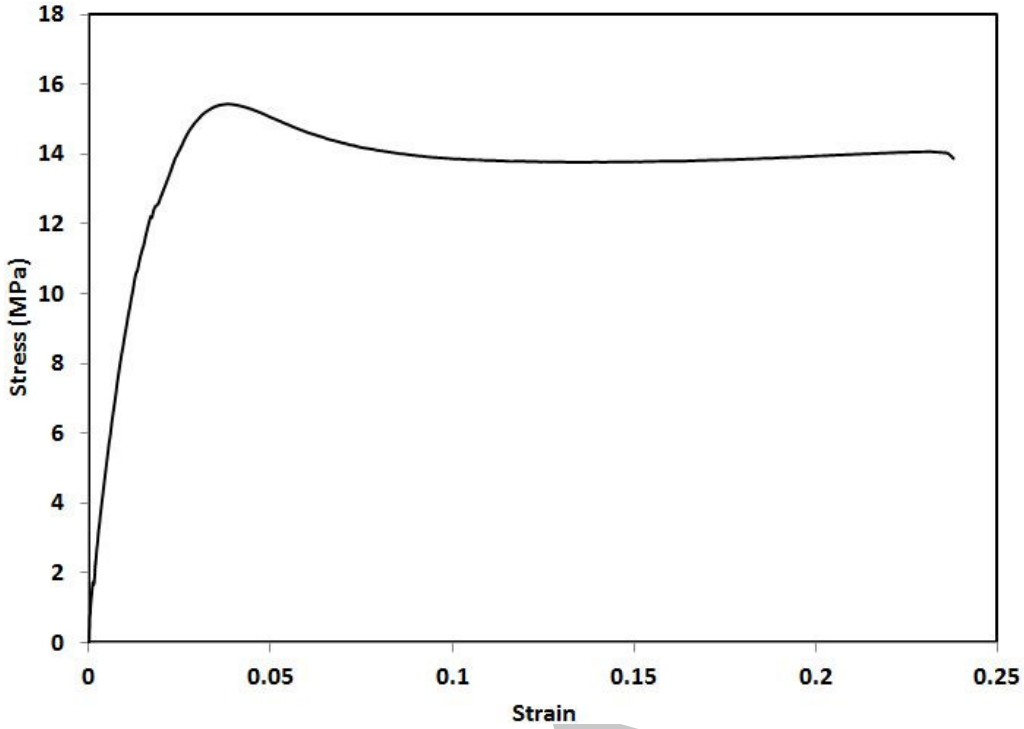

Fig 2. A typical engineering stress-strain curve of the epoxy matrix.

Table 1. Average material properties of employed E-glass fibers.

Elastic modulus (GPa)	Tensile strength (MPa)	Density (g/cm^3) [33]	Peak force (N)	Breakage displacement (mm)
53.6	1000	2.58	42.6	4.4

Table 2. Mechanical properties of the employed epoxy matrix.

Elastic modulus (MPa)	Tensile strength (MPa)	Density of CY-219 epoxy (g/cm3)	Density of HY-5161 hardener (g/cm3)	Density of matrix (g/cm3)
1020	15.1	1.1	1.0	1.067

2.2. Specimen manufacturing

Two different types of unstiffened (US) and lozenge grid-stiffened (GS) cylindrical composite shells were manufactured by using a filament winding machine. In order to fabricate the specimens, at first a cylindrical polyethylene mold, as the outer part of the mold, was machined which contains 3 clock-wise and 3 counter clock-wise helical grooves. The outer part of the mould is made from many separated pieces screwed onto the inner part of the mould as can be seen in Fig. 3a. The cross section of helical grooves and therefore the cross section of the grids was a square each side 6 mm. The final manufactured mold system is shown in Fig. 3a and can be used several times. The mold was placed on the filament machine mandrel which had two different adjustable rotational and horizontal movements. Table 3 tabulates the geometrical dimensions of the mold system.

Table 3. Geometrical dimensions of the mold system.

Length of the inner mold (mm)	Length of the outer grooved mold (mm)	Groove pitch (mm)	Groove cross-section (mm^2)
410	360	720	6×6

For manufacturing the specimens, at first, the grooves were filled by E-glass fibers impregnated by matrix in order to produce the helical grids, by using an especial feeder which guides three sets of glass fibers with three fibers in each feeder's hole (fissure). After filling the grooves in 80 back and forth movements, the outer shell of the specimens was wound around the whole filled mold with a winding angle of ± 62°. The outer shell was wound by 80 back and forth winding movements. Fig. 4 depicts the manufacturing processes of the specimens. Afterwards, the whole system of mold and specimen were placed on a motor shaft and the specimens were cured at room temperature. Finally, after separating the inner and outer parts of the mold by using an especial fixture shown in Fig. 3b, manufacturing of the grid-stiffened specimen was completed. Geometrical characteristics of the final specimens and indenters are shown in Table 4. Fig. 5 illustrates the fabricated unstiffened and lozenge grid-stiffened specimens with an outer shell thickness of nearly 1 mm.

Table 4. Geometrical characteristics of the final specimens and indenters.

Shell Type*	Part no.	Inner diameter of the outer shell (mm, ±1)	Shell thickness (mm, ±0.1)	Length (mm, ±1)	Mass (g, ±0.1)	Indenter type (diameter in mm)
US	1	160	1.5	344	294.9	Cylindrical (90)
	2				290.7	
GS	1				449.7	
	2				435.3	
	3				424.3	
USF	1				291.4	Flat platens
	2				288.3	
GSF	1				440.7	
	2				417.8	
	3				441.4	

*:
US: Unstiffened specimens indented by cylindrical indenter
GS: Grid-Stiffened specimens indented by cylindrical indenter
USF: Unstiffened specimens compressed between tow rigid flat platens
GSF: Grid-Stiffened specimens compressed between tow rigid flat platens

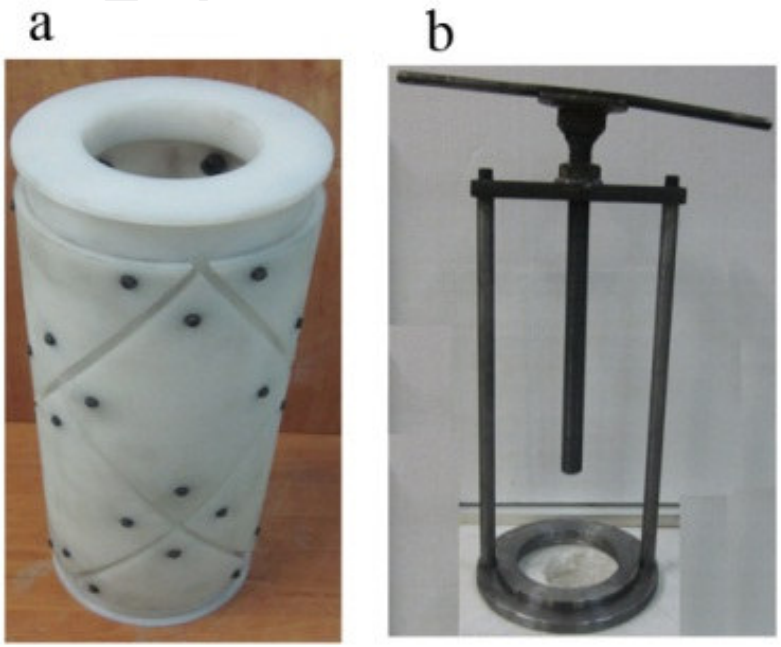

Fig 3. The complete inner and outer mold system (a) and the special fixture used to separate the specimen and the outer grooved mold from inner mold (b).

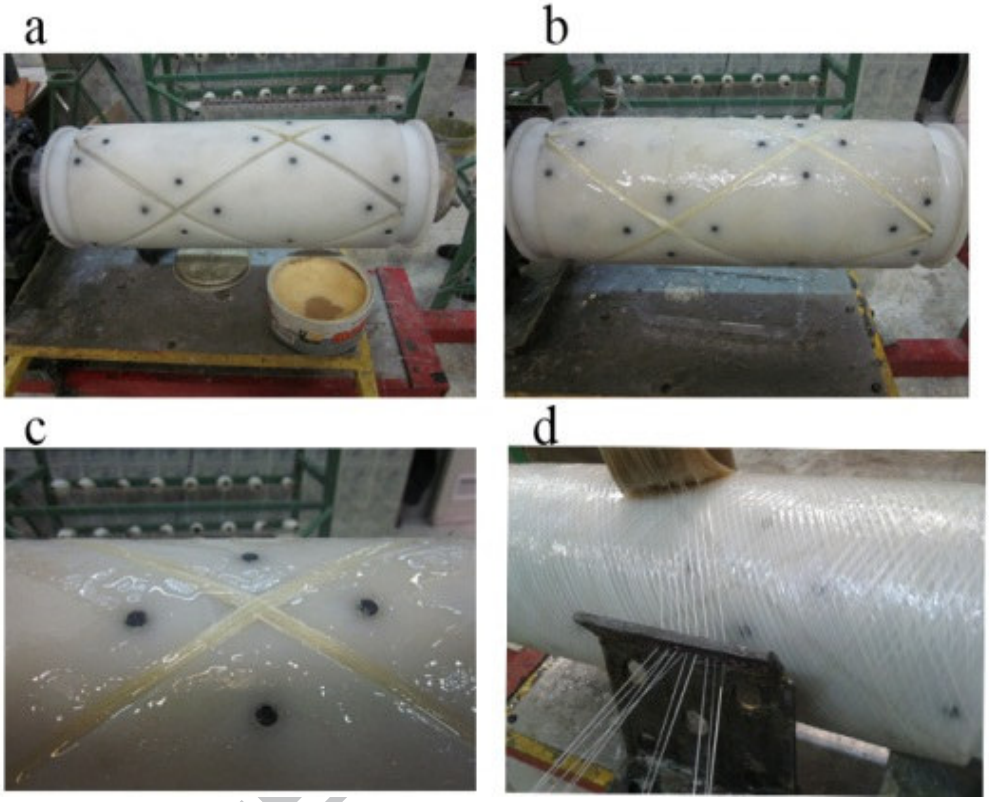

Fig 4. Manufacturing processes of the grid-stiffened tube, before starting the process (a) after manufacturing the lozenge grids (b) the close view of the grid intersection (c) during the outer shell winding (d).

Fig 5. The fabricated unstiffened (US) (a) and grid-stiffened (GS) (b) composite shells.

2.3. Compression tests

Two kinds of unstiffened (US) and grid-stiffened (GS) structures were compressed using either two flat steel platens or a flat steel platen with a rigid cylindrical steel indenter with outer diameter of 90 mm. In the second testing procedure, the rigid cylindrical indenter was limited to have horizontal movement. For the sake of symmetric loading condition, in both of testing procedures, the specimen was placed under the platens and indenter in such a manner that the two adjacent grid intersections were adjusted in both sides of the compression punch equally (i.e. the initial loading point). Fig. 6 shows the specimen GS-1 and the closed view of the initial loading point. An Instron universal testing machine was employed to carry out the experiments with a quasi-static displacement rate of 10 mm/min. Each testing procedure was repeated two or three times in order to mitigate the probable affecting defects which may be produced by manufacturing or testing imperfections. The average data of repeated tests are reported in this article.

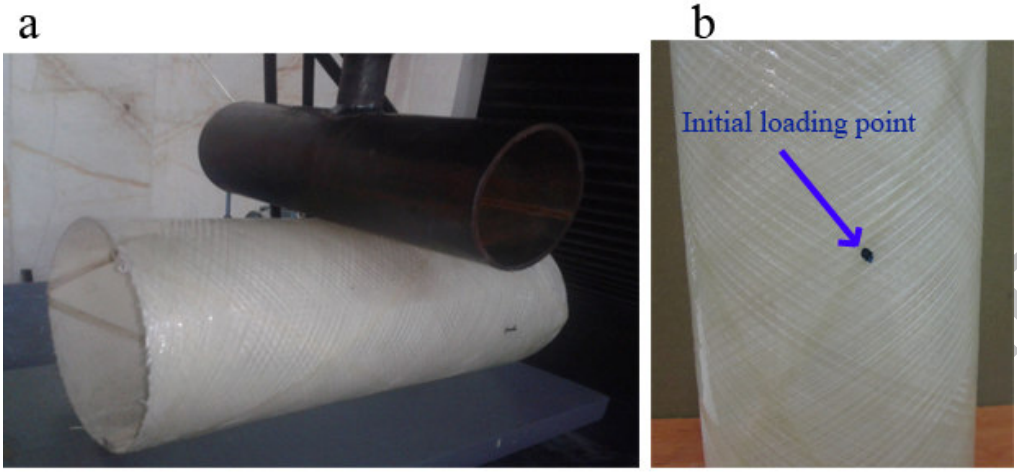

Fig 6. The GS specimen indented by the rigid cylindrical indenter (a) and the close view of the initial loading point (b).

3. Results and discussion

Load-displacement diagram of the energy absorbing structures is the key factor in their design and application. Structures with a high mean crushing load and a low initial peak load are known as the most efficient energy absorbers. Thus, in this section the crushing behavior and consequently, the load-displacement diagrams of the tested specimens are discussed.

3.1. Compression between a flat platen and a rigid cylindrical indenter

The load-displacement diagrams of the unstiffened and grid-stiffened specimens indented by the rigid cylindrical indenter are shown in Fig. 7. In order to show the variation of the actual data obtained in repeated tests, in this figure all three data with their average for grid-stiffened specimens (GS-1, GS-2, GS-3 and GS) are sketched. Also, all two load-displacement curves with their average for unstiffened specimens (US-1, US-2 and US) are plotted in this figure.

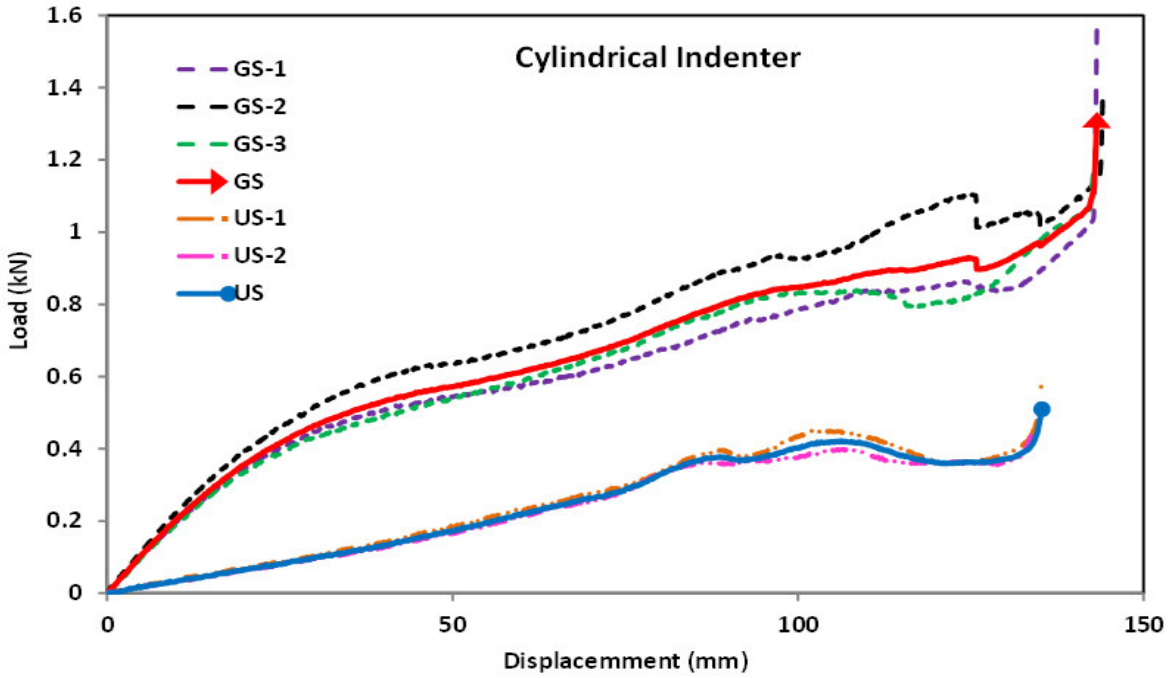

Fig 7. Load-displacement diagrams of the US and GS specimens compressed between a rigid cylindrical indenter and a flat platen.

As can be seen from the Figure 7, the grid-stiffened specimen has a higher contact force during the whole indentation stroke. This can be explained by this fact that the existence of the lozenge grids leads to more material contribution in the compression process of the stiffened specimen than the unstiffened one. In other words, in the indentation process of the grid-stiffened cylindrical shells, in contrast with the unstiffened specimens, the grid stiffeners distribute the local contact force to the whole length of the specimen. This process was observed in the experiments and can be seen in Fig. 8. Also, according to Fig. 7, in the elastic part of the diagram, the slope of the load-displacement curves of the grid-stiffened shell is

steeper than the slope of the unstiffened shell, which means a higher stiffness of the stiffened shell.

During the experiments, specimens made some cracking sounds which can be corresponded to the load downfalls of the load-displacement diagrams (Fig. 7). During the compression processes, two local plastic hinges were produces at both sides of unstiffened shells and under the indentation area, while two plastic hinges were produced at full length on each side of the grid-stiffened specimens.

Also, it is worth notice that in the grid-stiffened specimens, after removing the compression load, the specimens sprung back and formed an elliptical shape cross-section, while no spring back observed in the unstiffened specimens.

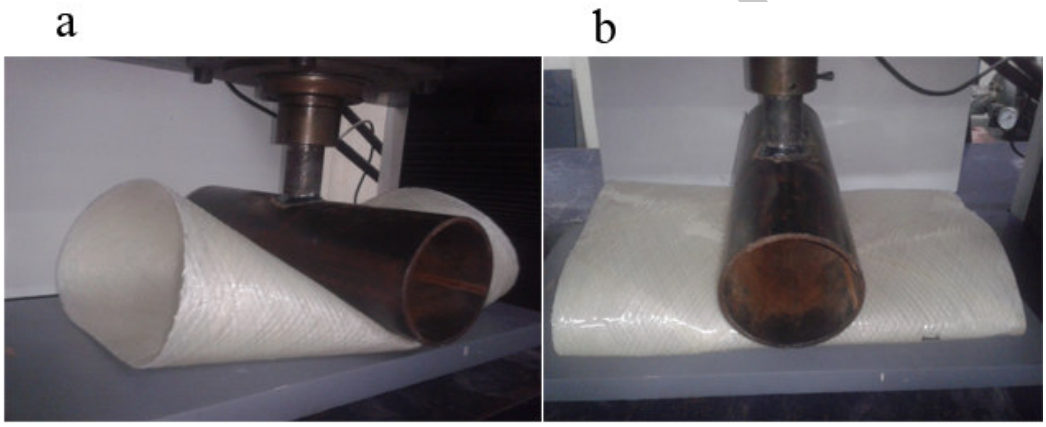

Fig 8. Final deformation of the US (a) and GS (b) specimens under indentation.

The energy-displacement and the specific energy-displacement of the US and GS specimens indented by the cylindrical indenter are depicted in Figs. 9 and 10, respectively. The value of energy is manually calculated from the force-displacement data obtained from the machine by integrating the area under the load-displacement curve. It can be seen from these figures that the presence of the grid stiffeners leads to higher energy absorption as well as specific energy absorption, when indented by a cylindrical indenter laterally.

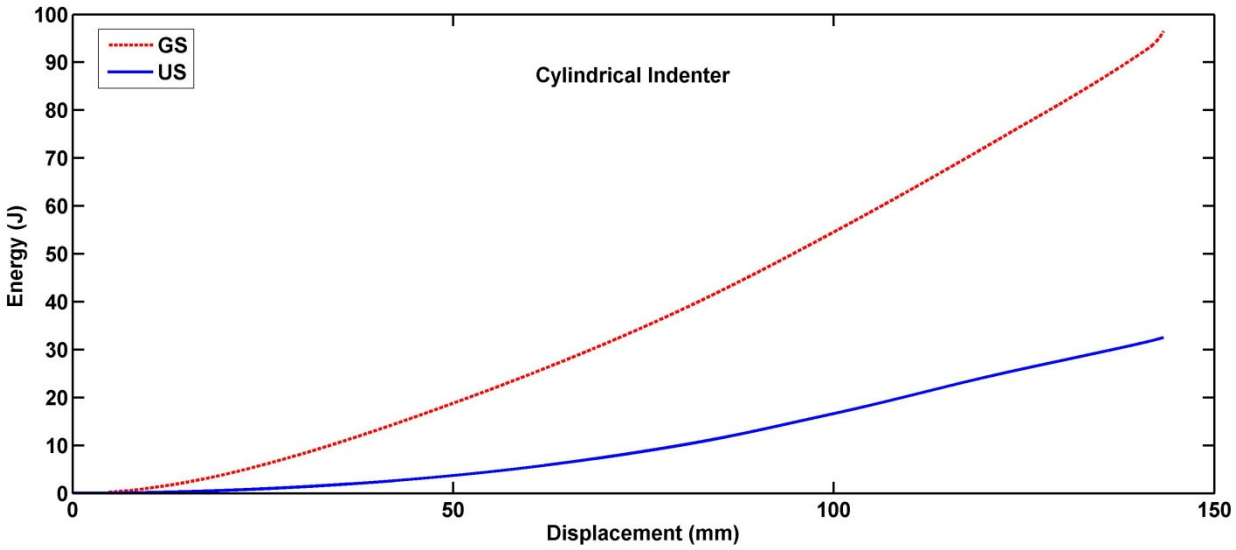

Fig 9. Energy absorption diagrams of the US (a) and GS (b) specimens versus compressed lateral displacement under rigid cylindrical indenter.

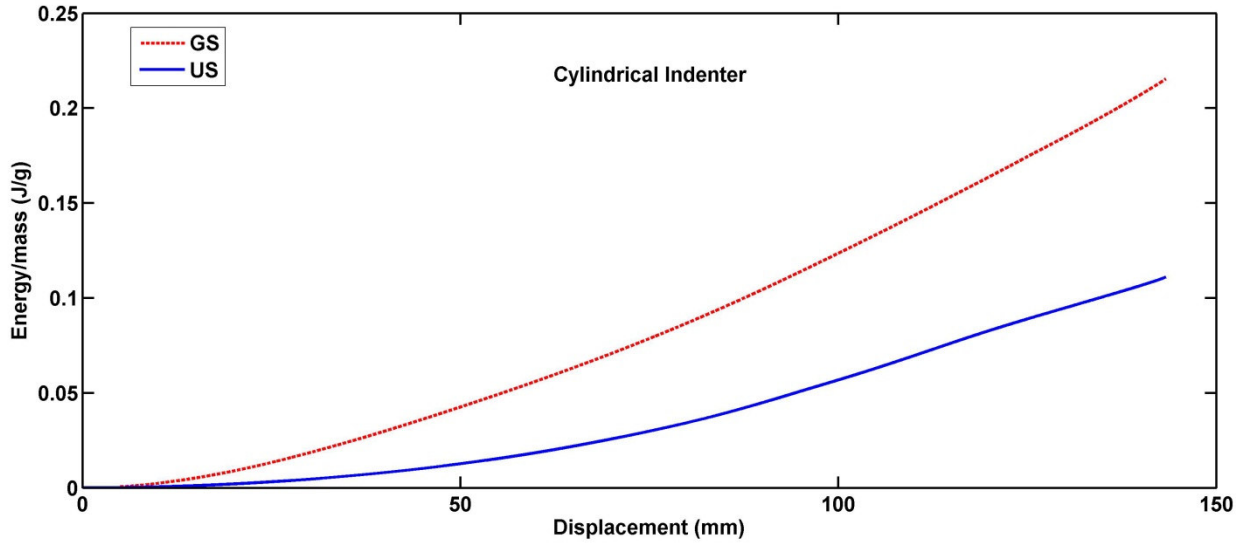

Fig 10.Specific energy absorption diagrams of the US and GS specimens versus compressed lateral displacement under rigid cylindrical indenter.

3.2. Compression between two rigid flat steel platens

In order to investigate the contact force and the energy absorption in the flattening process of the USF and GSF specimens, in this section the two types of specimens are compressed between two rigid flat steel platens. Fig. 11 shows the unstiffened and grid-stiffened specimens during the compression between two rigid steel platens.

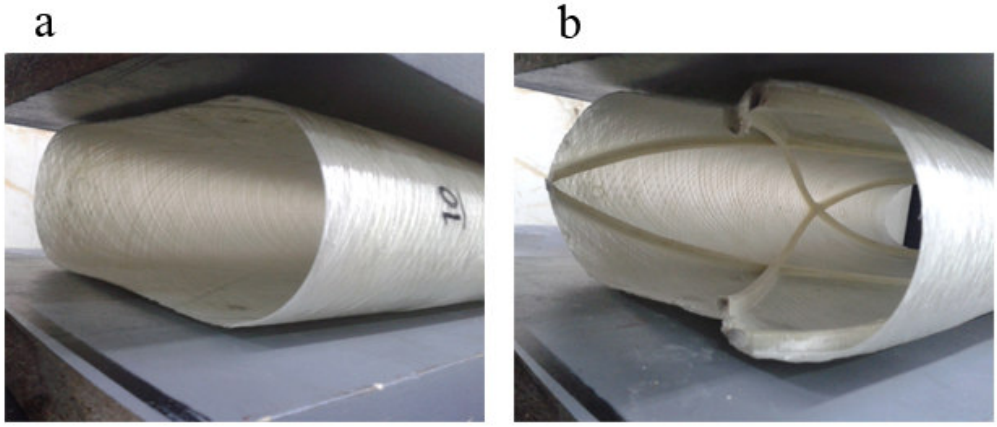

Fig 11. Unstiffened (a) and grid-stiffened (b) specimens during flattening process between two flat steel platens.

In these cases, two plastic hinges produced in both the front and back sides of the specimens. During the tests, it was observed that in both sides of the grid-stiffened shells, the helical ribs separated from the outer cylindrical shell by occurrence of tearing process in the outer shell. The load-displacement and variation of the energy absorption of these experiments are shown in Figs. 12 and 13, respectively.

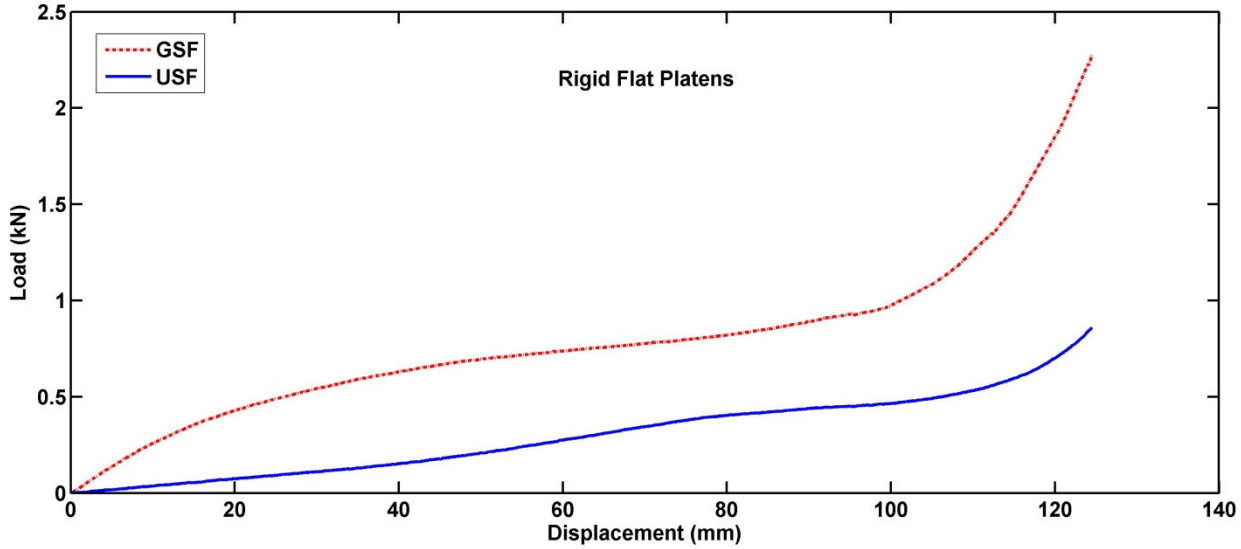

Fig 12. Load-displacement diagrams of the USF and GSF specimens compressed between two rigid flat steel platens.

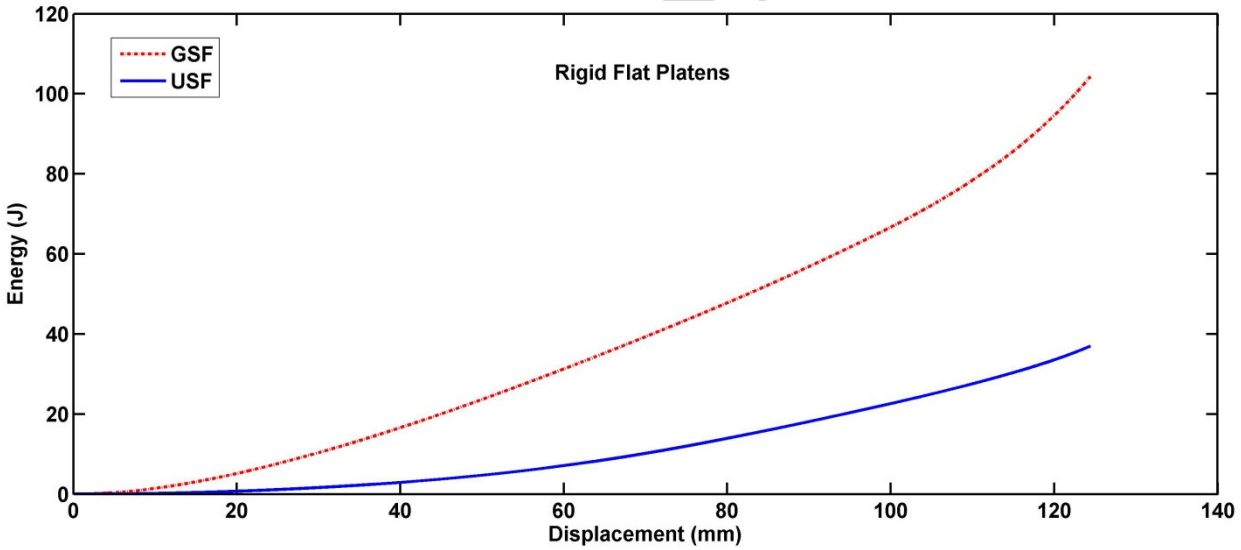

Fig 13. Energy absorption versus lateral displacement of the USF and GSF specimens compressed between two rigid flat steel platens.

As can be seen from Figs. 12 and 13, the grid stiffened specimens are stiffer than the unstiffened specimens and in the same lateral displacement they can absorb more than twice energy in comparison with the unstiffened specimens. The

specific energy absorption diagrams versus the lateral displacement of the USF and GSF composite shells are depicted in Fig. 14.

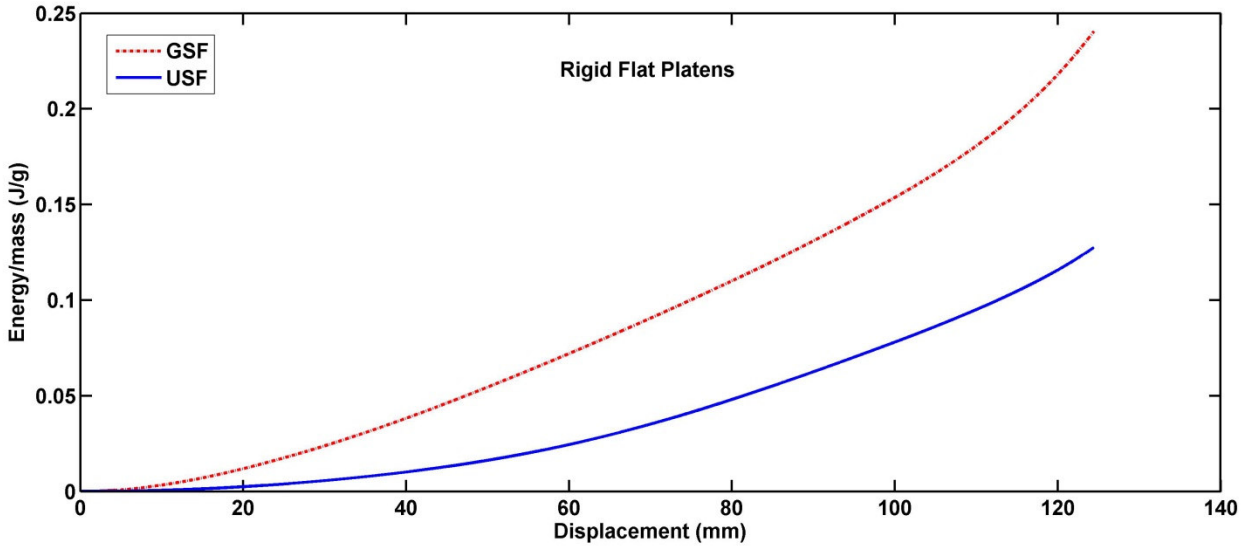

Fig 14. Specific energy absorption diagrams of the USF and GSF specimens versus lateral displacement compressed between two rigid flat steel platens.

3.3. Effect of loading condition

In order to investigate the effect of loading condition on the deformation behavior and energy absorption capacity of the composite shells, Figs. 15 and 16 respectively show the load-displacement diagrams of the grid-stiffened and unstiffened composite shells.

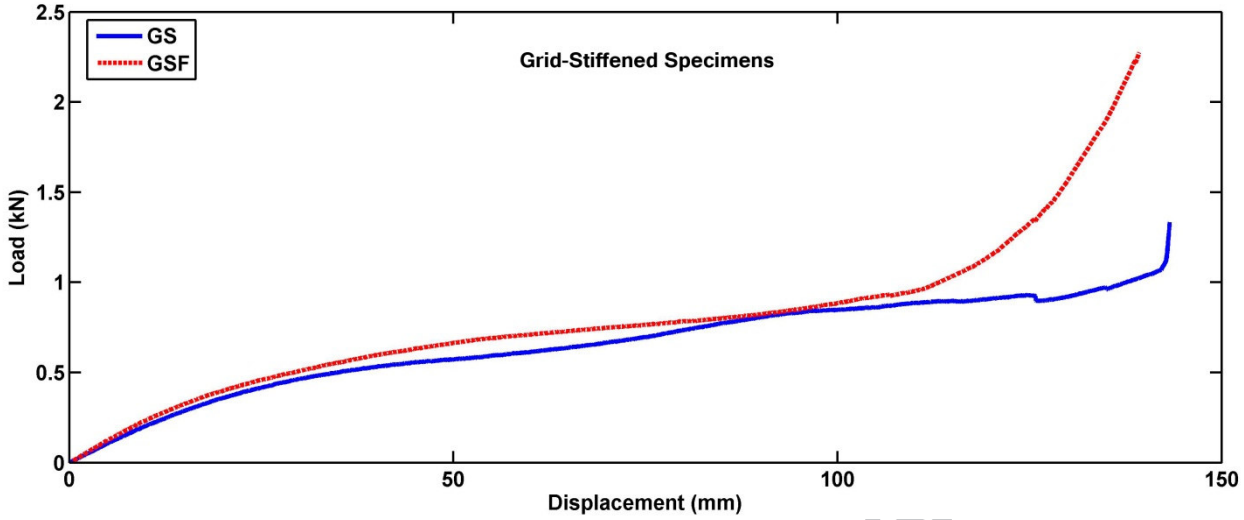

Fig 15. Load-displacement diagrams of the GS specimens compressed in two different loading conditions.

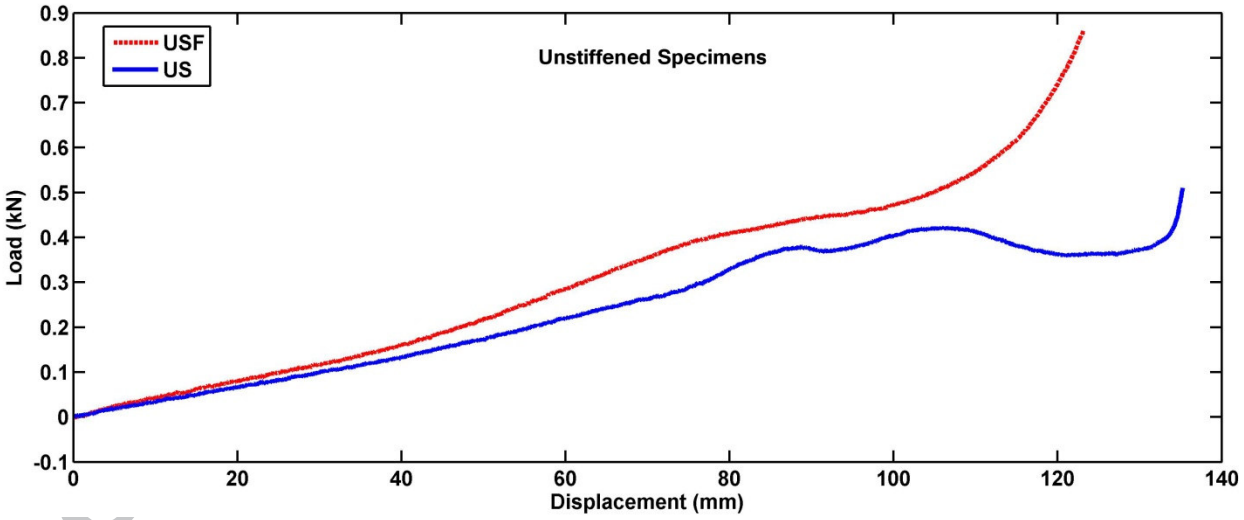

Fig 16. Load-displacement diagrams of the US specimens compressed in two different loading conditions.

According to the figures, load downfalls appeared in the load-displacement diagrams of the US and GS specimens when indented by rigid cylindrical indenter, while no load downfall occurred in both US and GS specimens when indented by two rigid flat platens. These downfalls can be attributed to the sever deformation

under the punch area which can be corresponded to the cracking sound heard during the experiments.

In order to have a better comparison, Figs. 17 and 18 show the specific energy absorption (SEA) of the US and GS specimens under two different mentioned loading conditions. These figures illustrate the average values of specific absorbed energy by all tested specimens in two different lateral displacements of 40 mm (δ/D= 0.25) and 100 mm (δ/D= 0.625), respectively.

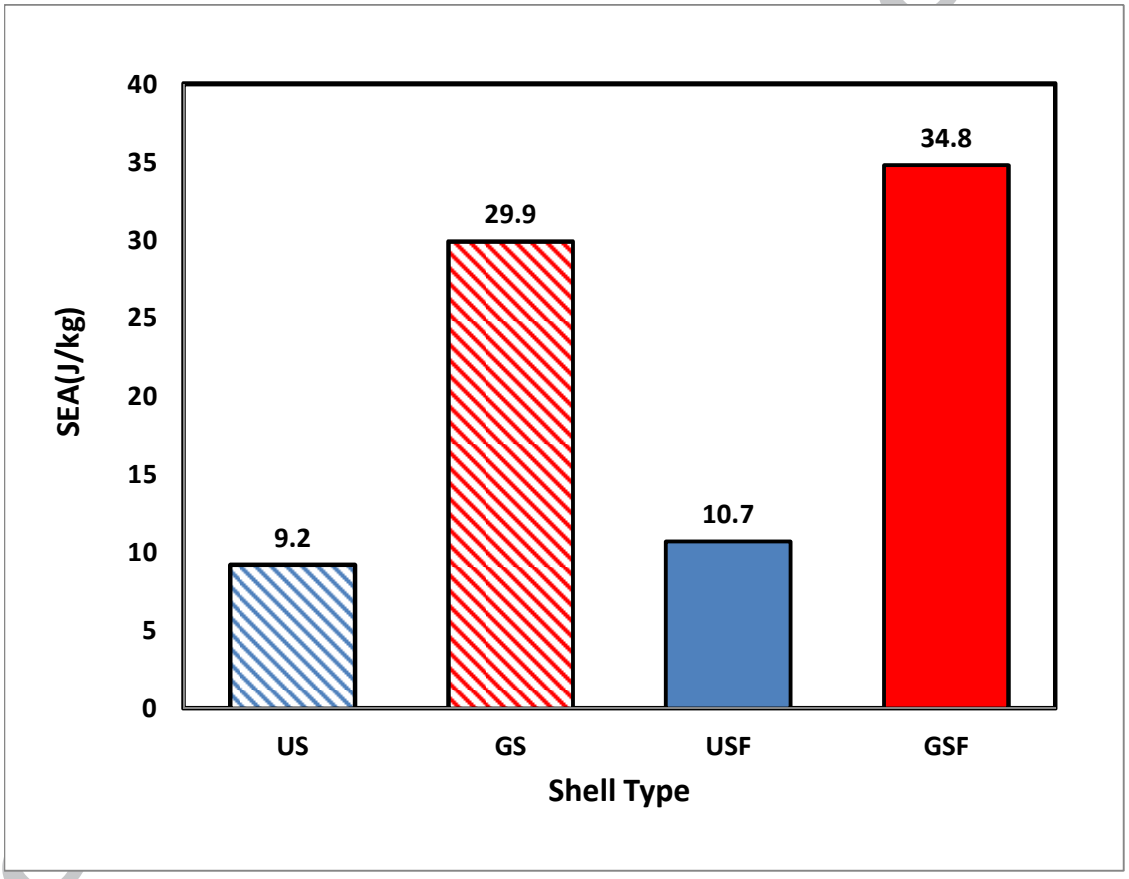

Fig 17. Specific absorbed energy of the tested specimens in a lateral displacement of 40 mm (δ/D= 0.25).

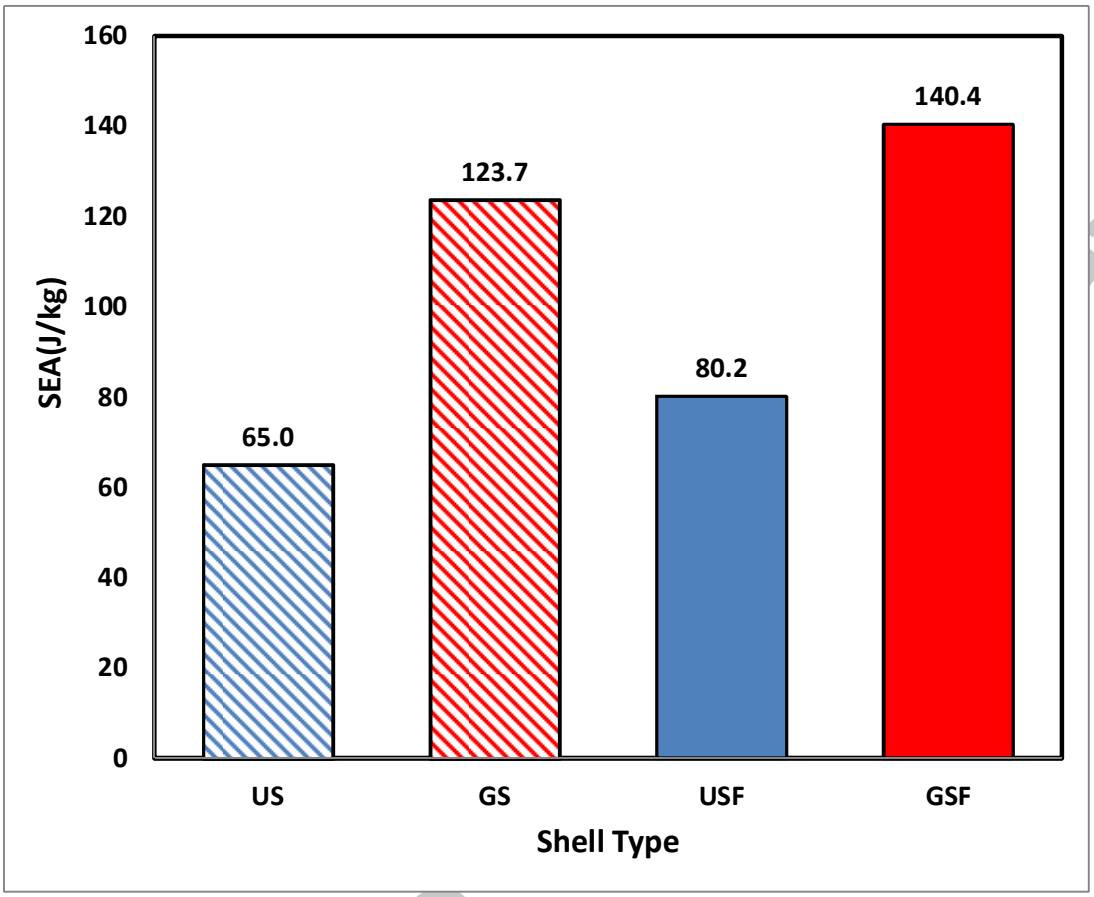

Fig 18. Specific absorbed energy of the tested specimens in a lateral displacement of 100 mm (δ/D= 0.625).

Based on the previous research on the grid-stiffened composite cylindrical shells [32], existence of the grid stiffeners negatively affected the specific buckling load of the structure. In contrast, based on the above figures, it can be obviously seen that existence of the grid stiffeners leads to a remarkable increase in the specific energy absorption.

Also, it can be seen that the grid stiffened composite shells compressed between two rigid flat platens have the maximum specific energy absorption in the whole compression process, while the unstiffened composite shells indented by the rigid cylindrical indenter have the minimum value of the specific energy absorption. It should be noted that, the effect of the grid stiffeners on the stiffness, contact force and consequently on the energy absorption capacity of the composite shells is more

significant when the structure is compressed locally between a rigid cylinder and a rigid flat platen than between two rigid flat platens. Furthermore, it can be realized from the results that the effect of the stiffeners on the stiffness, contact force and energy absorption capacity of the structures is more significant in the elastic deformation stage of the compression process, i.e. in the lateral displacement of 40 mm ($\delta/D= 0.25$).

Conclusion

In this study, unstiffened and lozenge grid-stiffened composite cylindrical shells were investigated experimentally. The composite structures were compressed in two different loading conditions; between two rigid flat platens and, a rigid flat platen with a rigid cylindrical indenter. The experimental results showed that existence of the grid stiffeners led to distribution of the lateral load along the whole length of the specimen, especially when indented locally by cylindrical indenter. Also, it was observed that the grid-stiffened shells were stiffer than the unstiffened shells, especially in the elastic stage of the deformation. The stiffness, contact force and consequently the energy absorption capacity of the grid-stiffened structures were compared with the unstiffened shells. The results showed that the stiffness, contact force and the energy absorption capacity of the grid-stiffened specimens were significantly higher than the unstiffened ones in two different loading conditions. Experimental data revealed that existence of the grid stiffeners led to an increase in the specific energy absorption of the composite cylindrical shells.

In summary, the grid-stiffened structures had the highest specific energy absorption capacity when compressed by two rigid flat platens, while the unstiffened shells had the least capacity to absorb energy when indented by the rigid cylindrical indenter.

References

[1] Niknejad A, Abedi MM, Liaghat GH, Zamani Nejad M. Prediction of the mean folding force during the axial compression in foam-filled grooved tubes by theoretical analysis. Materials & Design. 2012;37:144-51.

[2] Niknejad A, Liaghat GH, Moeinifard M. Experimental Investigation of the Rubber-Filled Tubes in the Tube Inversion Process. Advanced Materials Research. 2012;445:33-8.

[3] Niknejad A, Liaghat GH, Moslemi Naeini H, Behravesh AH. Theoretical and experimental studies of the instantaneous folding force of the polyurethane foam-filled square honeycombs. Materials & Design. 2011;32:69-75.

[4] Niknejad A, Moeinifard M. Theoretical and experimental studies of the external inversion process in the circular metal tubes. Materials & Design. 2012;40:324-30.

[5] Salehghaffari S, Tajdari M, Panahi M, Mokhtarnezhad F. Attempts to improve energy absorption characteristics of circular metal tubes subjected to axial loading. Thin-Walled Structures. 2010;48:379-90.

[6] Sohn SM, Kim BJ, Park KS, Moon YH. Evaluation of the crash energy absorption of hydroformed bumper stays. Journal of Materials Processing Technology. 2007;187–188:283-6.

[7] Alghamdi AAA. Collapsible impact energy absorbers: an overview. Thin-Walled Structures. 2001;39:189-213.

[8] Olabi AG, Morris E, Hashmi MSJ. Metallic tube type energy absorbers: A synopsis. Thin-Walled Structures. 2007;45:706-26.

[9] Olabi AG, Morris E, Hashmi MSJ, Gilchrist MD. Optimised design of nested circular tube energy absorbers under lateral impact loading. International Journal of Mechanical Sciences. 2008;50:104-16.

[10] Morris E, Olabi AG, Hashmi MSJ. Analysis of nested tube type energy absorbers with different indenters and exterior constraints. Thin-Walled Structures. 2006;44:872-85.

[11] Morris E, Olabi AG, Hashmi MSJ. Lateral crushing of circular and non-circular tube systems under quasi-static conditions. Journal of Materials Processing Technology. 2007;191:132-5.

[12] Niknejad A, Elahi SA, Liaghat GH. Experimental investigation on the lateral compression in the foam-filled circular tubes. Materials & Design. 2012;36:24-34.

[13] Niknejad A, Elahi SM, Elahi SA, Elahi SA. Theoretical and experimental study on the flattening deformation of the rectangular brazen and aluminum columns. Archives of Civil and Mechanical Engineering. 2013;13:449-64.

[14] Niknejad A, Rahmani DM. Experimental and theoretical study of the lateral compression process on the empty and foam-filled hexagonal columns. Materials & Design. 2014;53:250-61.

[15] Hall IW, Guden M, Claar TD. Transverse and longitudinal crushing of aluminum-foam filled tubes. Scripta Materialia. 2002;46:513-8.

[16] Fan Z, Shen J, Lu G. Investigation of Lateral Crushing of Sandwich Tubes. Procedia Engineering. 2011;14:442-9.

[17] Taher ST, Zahari R, Ataollahi S, Mustapha F, Basri S. A double-cell foam-filled composite block for efficient energy absorption under axial compression. Composite Structures. 2009;89:399-407.

[18] Palanivelu S, Paepegem WV, Degrieck J, Vantomme J, Kakogiannis D, Ackeren JV, et al. Crushing and energy absorption performance of different geometrical shapes of small-scale glass/polyester composite tubes under quasi-static loading conditions. Composite Structures. 2011;93:992-1007.

[19] Chiu LNS, Falzon BG, Ruan D, Xu S, Thomson RS, Chen B, et al. Crush responses of composite cylinder under quasi-static and dynamic loading. Composite Structures. 2015;131:90-8.

[20] Tarlochan F, Ramesh S, Harpreet S. Advanced composite sandwich structure design for energy absorption applications: Blast protection and crashworthiness. Composites Part B: Engineering. 2012;43:2198-208.

[21] Mahdi E, Sebaey TA. An experimental investigation into crushing behavior of radially stiffened GFRP composite tubes. Thin-Walled Structures. 2014;76:8-13.

[22] Gupta NK, Abbas H. Lateral collapse of composite cylindrical tubes between flat platens. International Journal of Impact Engineering. 2000;24:329-46.

[23] Calme O, Bigaud D, Hamelin P. 3D braided composite rings under lateral compression. Composites Science and Technology. 2005;65:95-106.

[24] Abosbaia AS, Mahdi E, Hamouda AMS, Sahari BB, Mokhtar AS. Energy absorption capability of laterally loaded segmented composite tubes. Composite Structures. 2005;70:356-73.

[25] Mahdi E-S, El Kadi H. Crushing behavior of laterally compressed composite elliptical tubes: Experiments and predictions using artificial neural networks. Composite Structures. 2008;83:399-412.

[26] Niknejad A, Assaee H, Elahi SA, Golriz A. Flattening process of empty and polyurethane foam-filled E-glass/vinylester composite tubes – An experimental study. Composite Structures. 2013;100:479-92.

[27] Hafeez F, Almaskari F. Experimental investigation of the scaling laws in laterally indented filament wound tubes supported with V shaped cradles. Composite Structures. 2015;126:265-84.

[28] D. Kim T. Postbuckled behavior of composite isogrid stiffened shell structure. Advanced Composite Materials. 2000;9:253-63.

[29] Kidane S. Buckling analysis of grid stiffened composite structures: Faculty of the Louisiana State University and Agricultural and Mechanical College in partial fulfillment of the requirements for the degree of Master of Science in Mechanical Engineering in The Department of Mechanical Engineering By Samuel Kidane B. Sc., Addis Ababa University, 2002.

[30] Zhang Z, Chen H, Ye L. Progressive failure analysis for advanced grid stiffened composite plates/shells. Composite Structures. 2008;86:45-54.

[31] Buragohain M, Velmurugan R. Study of filament wound grid-stiffened composite cylindrical structures. Composite Structures. 2011;93:1031-8.

[32] Yazdani M, Rahimi H, Khatibi AA, Hamzeh S. An experimental investigation into the buckling of GFRP stiffened shells under axial loading. Scientific Research and Essay. 2009;4:914-20.

[33] Wallenberger FT, Bingham PA. Fiberglass and glass technology: energy-friendly compositions and applications: Springer Science & Business Media, 2009.